Instability of a multimode oscillation in a photorefractive ring oscillator

Zhuang Jun*
Shanghai Institute of Optics and Fine Mechanics, Academia Sinica, P. O. Box 800-211, Shanghai 201800, China

Tan Weihan
Shanghai University, Shanghai Institute of Optics and Fine Mechanics, Academia Sinica, P. O. Box 800-211, Shanghai 201800, China

(Received 7 July 1995)

A theory of multimode oscillation in an optical unidirectional ring resonator with photorefractive gain was given in the weak-field limit, in which the mode coupling is considered carefully. The characteristics of single-mode oscillation in steady state were analyzed in detail, especially when the externally applied dc electric field is not zero. By numerical simulation, we investigated a three-mode oscillation and observed instability phenomena which are similar to the periodic oscillation of several transverse family modes observed in experiment. [S1050-2947(96)01011-6]

PACS number(s): 42.65.Hw, 42.65.Sf, 05.45.+b

I. INTRODUCTION

In the study of the spatiotemporal dynamics of nonlinear optical systems, most experimental and theoretical studies are devoted to lasers [1–4]. Recently there has also been an increase of interest in photorefractive oscillators (PRO's) for their rich spatiotemporal phenomena, for example, periodic alternation of transverse modes, optical vortices, and spatiotemporal chaos [8–10]. So PRO provides another good physics model for studying spatiotemporal behavior of nonlinear optical systems. However, even in a PRO operating in the weakly multimode case, the spatiotemporal instabilities have not been given completely by theory, although some characteristics and phenomena such as multimode competition, spatiotemporal periodic behavior resulting from the frequency beating between two different transverse modes, have been considered [11–14].

There are generally two different research methods to study spatiotemporal dynamics of lasers. One is a global approach similar to that used in hydrodynamics [15,16]. Another is decomposition of the electric field on the modes of the empty cavity [2–7]. In this paper, we pursue the latter research line with the derivation following procedures in literature [2] for a laser. Neglecting the depletion of the pump beam in the weak-field limit, we give the multimode oscillation equation in Sec. II for a PRO in which the influence of an externally applied dc electric field is included. The uniform field limit which has already played a useful role in studying lasers is also introduced to simplify the equations. In Sec. III we give some characteristics of single-mode oscillation in steady state, particularly the intensity and frequency pulling when the externally applied dc electric field is not equal to zero. Finally, multimode oscillation is discussed in Sec. IV, in which a three-mode oscillation is studied by numerical simulation. Because of the mode coupling in degenerate or quasidegenerate states, some instability phenomena such as periodic alteration of the transverse modes [8,10] are observed. In nondegenerate states, however, the system can be described by the Lotka-Volterra equation. The conclusions are presented in Sec. V.

II. MULTIMODE OSCILLATION EQUATION FOR A PRO IN THE WEAK-FIELD LIMIT

We know that the volume index grating induced by two interfering light waves in a photorefractive medium is generally accompanied by an energy redistribution between these two waves. This kind of intensity transfer (or beam coupling) is due to a finite spatial phase shift ψ between the index grating and the interference pattern, and when this phase shift $\psi=\pi/2$, the maximum energy transfer is obtained. The phase shift ψ includes a constant phase shift ϕ_0 related to the nonlocal response of the medium under fringe illumination and the phase shift introduced artificially by external means (e.g., moving medium, fringe displacement), where ϕ_0 is dependent on the dc electric field (E_0) applied on the photorefractive medium and decreases from $\pi/2$ to 0 as the field (E_0) increases from zero [17,18]. This means that we can study the characteristics of the PRO under different dc electric fields E_0 by changing the parameter ϕ_0 in the equations.

A typical photorefractive oscillator based on the two-wave-mixing process is presented in Fig. 1. It is composed of a ring cavity and a photorefractive medium which is placed between two spherical mirrors M_1 and M_2. M_1 is a total reflection mirror, and the reflectivity of M_2 is R. The total cavity length is L, the length of the medium is l_A. We assume for simplicity that both waves (pump and signal beams in Fig. 1) have the same state of polarization and the pump beam is a plane wave:

$$E_p(t,\vec{r})=A_p e^{[i(\vec{k}_p\cdot\vec{r}-\omega_p t)]}+\text{c.c.} \tag{1}$$

When the PRO operates in the weak-field limit, i.e., the intensity of the signal beam is far less than that of the pump beam, $I_s \ll I_p$, the depletion of the pump beam can be ne-

*Present address: Department of Physics, FuDan University, 200433 Shanghai, China.

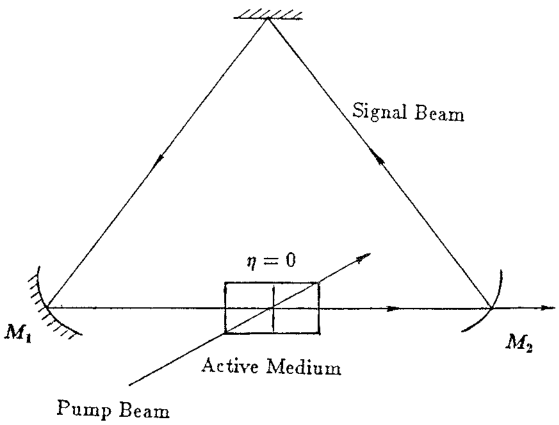

FIG. 1. Schematic representation of a unidirectional ring photorefractive oscillator with two spherical mirrors. The length of the ring is L. $\eta=0$ indicates the origin of the longitudinal coordinate system, and η measures various longitudinal positions of relevance to our discussion, in units of L. The length of the active medium is l_A.

glected, and so A_p in Eq. (1) is written as a constant irrelevant to the time and space. The signal beam, however, should be a sum of modes:

$$E_s(t,\vec{r}) = \sum_j \overline{A_j}(t,\vec{r}) e^{[i(\vec{k}_j\cdot\vec{r}-\omega_j t)]} + \text{c.c.}, \tag{2}$$

where j indicates the different modes and ω_j are their operating frequency (unknown). Drawing the fast varying factor $e^{[i(\vec{k}_c\cdot\vec{r}-\omega_c t)]}$ from the above equation, we can rewrite it to

$$E_s(t,\vec{r}) = A_s(t,\vec{r}) e^{[i(\vec{k}_c\cdot\vec{r}-\omega_c t)]} + \text{c.c.}, \tag{3}$$

where

$$A_s(t,\vec{r}) = \sum_j \overline{A_j}(t,\vec{r}) e^{\{i[(\vec{k}_j-\vec{k}_c)\cdot\vec{r}-(\omega_j-\omega_c)t]\}}.$$

ω_c (reference frequency) is the empty-cavity resonance frequency of one oscillating mode. From Eqs. (1) and (2) we can write out the interference pattern formed in the region of the medium:

$$I(t,\vec{r}) = I_0(t,\vec{r})[1 + M(t,\vec{r})], \tag{4}$$

where

$$I_0(t,\vec{r}) = I_p + I_s = |A_p|^2 + \sum_j |\overline{A_j}(t,\vec{r})|^2,$$

$$M(t,\vec{r}) = \sum_j M_j(t,\vec{r}) = \sum_j \frac{A_p\overline{A_j^*}(t,\vec{r})}{I_0(t,\vec{r})} e^{i(\vec{k}_{pj}\cdot\vec{r}-\delta_{pj}t)} + \text{c.c.},$$

$$\vec{k}_{pj} = \vec{k}_p - \vec{k}_j, \quad \delta_{pj} = \omega_p - \omega_j.$$

In Eq. (4) the interference patterns of the various modes with each other are neglected, because the index gratings arising from these patterns are much smaller than that caused by the interference of each mode with the pump beam in the weak-field limit [14]. In order to get the index grating $\Delta n(t,\vec{r})$ induced by the fringe illumination Eq. (4), we decompose the factor $A_pA_j^*(t,\vec{r})/I_0(t,\vec{r})$ of $M_j(t,\vec{r})$ by Fourier transform in transverse space:

$$\frac{A_p\overline{A_j^*}(t,\vec{r})}{I_0(t,\vec{r})} = \int d\vec{k}_{q'} C(t,z,\vec{k}_{q'}) e^{-i\vec{k}_{q'}\cdot\vec{r}} + \text{c.c.} \tag{5}$$

and

$$C(t,z,\vec{k}_{q'}) = \int d\vec{r}_{xy} \frac{A_p\overline{A_j^*}(t,\vec{r})}{I_0(t,\vec{r})} e^{i\vec{k}_{q'}\cdot\vec{r}_{xy}} + \text{c.c.},$$

where $\int d\vec{r}_{xy}$ indicates the integration in transverse space. Then the modulation $M_j(t,\vec{r})$ can be written as

$$M_j(t,\vec{r}) = \int d\vec{k}_{q'} C(t,z,\vec{k}_{q'}) e^{-i\vec{k}_{q'}\cdot\vec{r}} e^{i(\vec{k}_{pj}\cdot\vec{r}-\delta_{pj}t)} + \text{c.c.}$$

$$= \int d\vec{k}_q C(t,z,\vec{k}_q) e^{i(\vec{k}_{pq}\cdot\vec{r}-\delta_{pj}t)} + \text{c.c.},$$

$$\vec{k}_{pq} = \vec{k}_p - \vec{k}_q$$

where $\vec{k}_q = \vec{k}_j + \vec{k}_{q'}$. Noting that $[C(t,z,\vec{k}_q)e^{i(\vec{k}_{pq}\cdot\vec{r}-\delta_{pj}t)} + \text{c.c.}]$ can be regarded as the modulation of the pump beam with a uniform plane wave, we can write out the index grating $\Delta n_j(t,\vec{r})$ induced by $M_j(t,\vec{r})$ [17],

$$\Delta n_j(t,\vec{r}) = \frac{1}{\tau_0}\int_0^t dt' \; e^{-(t-t')/\tau_0} \times \left(\int d\vec{k}_q \gamma(k_{pq}) C(t',z,\vec{k}_q) e^{i(\vec{k}_{pq}\cdot\vec{r}-\delta_{pj}t')} \right) + \text{c.c.}, \tag{6}$$

where τ_0 is the dielectric relaxation time which depends on the light intensity and can be regarded approximately as a constant in the weak-field limit. $\gamma(k_{pq}) = \Delta n_s(k_{pq}) e^{i\phi_0(k_{pq})}$, Δn_s is the saturation value of the photoinduced index change, and ϕ_0 is a constant phase shift related to the nonlocal response of the medium under fringe illumination. The parameters Δn_s and ϕ_0 are all dependent on $k_{pq} = |\vec{k}_{pq}|$ (or the fringe spacing $\Lambda_{pq} = 2\pi/\kappa_{pq}$) besides the material properties of the crystal, e.g., the electro-optic coefficients [18]. From Eq. (5) we know that the spectrum $\delta k_{pq} = \delta k'_q$ around k_{pj} results from a transverse profile of the field $A_j(t,\vec{r})$ and can be estimated by $\delta k_{pq} \sim 1/w_0 \sim (1\text{ mm})^{-1}$ when the number of transverse modes is not very large in the oscillator, where w_0 is the beam waist. On the other hand, the fringe spacing in the two-wave-mixing process is typically on the order of 1 μm [17,18], i.e., $k_{pj} \sim 1/\Lambda_{pj} \sim (1\;\mu\text{m})^{-1} \gg \delta k_{pq}$. This means δk_{pq} around k_{pj} can be neglected and we have $\gamma(k_{pq}) \approx \gamma(k_{pj})$. Therefore Eq. (6) becomes

$$\Delta n_j(t,\vec{r}) \approx \gamma(k_{pj}) \frac{1}{\tau_0}\int_0^t e^{-(t-t')/\tau_0} \frac{A_p\overline{A_j^*}(t,\vec{r})}{I_0(t,\vec{r})} \times e^{i(\vec{k}_{pj}\cdot\vec{r}-\delta_{pj}t)} dt' + \text{c.c.}$$

and

$$\Delta n(t,\vec{r}) = \frac{1}{\tau_0}\sum_j \gamma(k_{pj})\int_0^t e^{-(t-t')/\tau_0}\frac{A_p\overline{A_j^*}(t,\vec{r})}{I_0(t,\vec{r})} \times e^{i(\vec{k}_{pj}\cdot\vec{r}-\delta_{pj}t)}dt' + \text{c.c.} \tag{7}$$

because the difference of the operating frequency ω_j for various modes is only a few Hz in PRO [12]. With the same consideration as above we have $\gamma(k_{pj}) \approx \gamma(k_{ps})$, where $k_{ps} = (\omega_p - \omega_s)/c$ and ω_s is the operating frequency of the mode whose empty-cavity resonance frequency is ω_c. Therefore Eq. (7) becomes

$$\Delta n(t,\vec{r}) = \Delta n_s(k_{ps})e^{i\phi_0(k_{ps})}\frac{1}{\tau_0}\int_0^t \frac{A_pA_s^*(t',\vec{r})}{I_0(t',\vec{r})} \times e^{i[(\vec{k}_p-\vec{k}_c)\cdot\vec{r}-\delta_{pc}t']}e^{-(t-t')/\tau_0}dt' + \text{c.c.}, \tag{8}$$

where Eq. (3) is used, and $\delta_{pc} = \omega_p - \omega_c$. Now, noticing that the refractive index of the photorefractive medium $n(t,\vec{r})$ should be written as $n = n_b + \Delta n(t,\vec{r})$, where n_b is the index in the absence of photorefractive coupling, and substituting Eqs. (1), (3), and (8) into the Maxwell equation with the slowly varying amplitude approximation, we get the following equation for the signal beam:

$$-i\frac{c^2}{2n_b^2\omega_c}\nabla_\perp^2 A_s + \frac{\partial A_s}{\partial t} + \left(\frac{c}{n_b}\right)\frac{\partial A_s}{\partial z} = i\frac{2\Delta n_s\pi}{\lambda}\left(\frac{c}{n_b}\right)I_p\frac{e^{-t/\tau_0}}{\tau_0}e^{-i(\phi_0+\delta_{pc}t)} \times\left(\int_0^t \frac{A_s}{I_0}e^{i\delta_{pc}t'}e^{t'/\tau_0}dt'\right), \tag{9}$$

where $\nabla_\perp^2 = \partial^2/\partial r^2 + (1/r)(\partial/\partial r) + (1/r^2)(\partial^2/\partial\phi^2)$. For simplicity, we introduce

$$E = A_s e^{i\delta_{sc}t},$$

$$P = -\left(\frac{e^{-t/\tau_0}}{\tau_0}\int_0^t \frac{A_s}{I_0}e^{i\delta_{pc}t'}e^{t'/\tau_0}dt'\right)e^{-i\delta_{pc}t},$$

where $\delta_{sc} = \omega_s - \omega_c$, $\delta_{ps} = \omega_p - \omega_s$, and adopting the new variables $\tau = (1/\tau_0)t$, $\eta = z/L$, $\rho = r(\pi n_b/L\lambda)^{1/2}$, Eq. (9) becomes

$$-\frac{i}{4}\nabla_\perp^2 E + \frac{\partial E}{\partial\eta} + \frac{1}{v}\frac{\partial E}{\partial\tau} = i\frac{\delta_1'}{v}E - \alpha LP,$$
$$\frac{\partial P}{\partial\tau} = -\left(\frac{E}{I_p+I_s} + (1+i\Delta_2')P\right), \tag{10}$$

where $\delta_1' = \delta_{sc}/\gamma_\perp$, $\Delta_2' = \delta_{ps}/\gamma_\perp$, $\gamma_\perp = 1/\tau_0$, $v = c/n_b\gamma_\perp L$, $\alpha = i(2\Delta n_s I_p\pi/\lambda)e^{-i\phi_0}$. Equation (10) is what we need to describe the signal beam varying with the time and space in the two-wave-mixing process.

The next step is to derive a set of equations for the field model amplitudes. For this purpose we decompose the field E and P on the empty-cavity modes, i.e., we consider the expansion

$$E(\rho,\phi,\eta,\tau) = \sum_m f_m(\eta,\tau)A_m(\rho,\phi,\eta),$$
$$P(\rho,\phi,\eta,\tau) = \sum_m q_m(\eta,\tau)A_m(\rho,\phi,\eta), \tag{11}$$

where $A_m(\rho,\phi,\eta)$ are the model functions. Index m indicates the different transverse mode (e.g., $m \to \{p,l,i\}$ for Gauss-Laguerre mode), and the index for longitude modes is omitted for convenience. Substituting Eq. (11) into Eq. (10) and using the orthogonality relation $\int_0^{2\pi}d\phi\int_0^\infty \rho\, d\rho\, A_{m_1}A_{m_2}^* = \delta_{m_1m_2}$, we obtain

$$\frac{\partial f_m}{\partial\eta} + \frac{1}{v}\frac{\partial f_m}{\partial\tau} = i\frac{\delta_1'}{v}f_m - \alpha Lq_m,$$
$$\frac{\partial q_m}{\partial\tau} = -\left((1+i\Delta_2')q_m + \frac{f_m}{I_p} - \frac{1}{I_p^2} \times\sum_{m_1,m_2} f_{m_1}|f_{m_2}|^2\Gamma_{m_1m_2m_2m}\right), \tag{12}$$

where we use the approximation $E/(I_p+I_s) \approx E/I_p - (E/I_p^2)I_s$ in the weak-field limit. $\Gamma_{m_1m_2m_2m}$ in Eq. (12) are the mode-mode coupling coefficients:

$$\Gamma_{m_1m_2m_2m} = \int_0^\infty \rho\, d\rho\int_0^{2\pi}d\phi\, A_{m_1}A_{m_2}A_{m_2}^*A_m^*(\rho,\phi,\eta).$$

On the other hand, the boundary conditions for model amplitudes $f_m(\eta,\tau)$ are [3]

$$f_m\left(-\frac{1}{2}\frac{l_A}{L},\tau\right) = \sqrt{R}e^{(-i\delta_m)}e^{[i\delta_1'\gamma_\perp(L-l_A)/c]} \times f_m\left(\frac{1}{2}\frac{l_A}{L},\tau-\gamma_\perp\frac{L-l_A}{c}\right), \tag{13}$$

where $\delta_m = (\omega_{nm} - \omega_c)/(c/L)$, index n indicates the different longitude modes. For convenience we transform them to standard periodicity form by introducing the new set of independent variables

$$\eta' = \frac{L}{l_A}\eta,$$

$$\tau' = \tau + \gamma_\perp\frac{L-l_A}{c}\left(\frac{L}{l_A}\eta + \frac{1}{2}\right)$$

and defining the new field amplitudes $\tilde{f}_m$,

$$f_m(\eta',\tau') = \tilde{f}_m(\eta',\tau')L_m(\eta'),$$

$$q_m(\eta',\tau') = \tilde{q}_m(\eta',\tau')L_m(\eta'),$$

where

$$L_m(\eta') = e^{\{-[\ln\sqrt{R} - i\delta_m + i\delta_1'\gamma_\perp(L-l_A)/c](\eta'+1/2)\}}. \tag{14}$$

Then the boundary conditions become

$$\widetilde{f}_m(-\tfrac{1}{2},\tau')=\widetilde{f}_m(\tfrac{1}{2},\tau') \tag{15}$$

and the equations for $\widetilde{f}_m(\eta',\tau')$ take the form

$$\frac{\partial\widetilde{f}_m}{\partial\eta'}+\frac{L\gamma_\perp}{c}\frac{\partial\widetilde{f}_m}{\partial\tau'}=\left(\ln\sqrt{R}-i\delta_m+i\delta_1'\gamma_\perp\frac{L}{c}\right)\widetilde{f}_m-\alpha l_A\widetilde{q}_m,$$

$$\frac{\partial\widetilde{q}_m}{\partial\tau'}=-\Bigg[(1+i\Delta_2')\widetilde{q}_m+\frac{\widetilde{f}_m}{I_p}-\frac{1}{I_p^2}\sum_{m_1,m_2}\Gamma_{m_1m_2m_2m}\times\left(\frac{L_{m_1}L_{m_2}L_{m_2}^*}{L_m}\right)\widetilde{f}_{m_1}|\widetilde{f}_{m_2}|^2\Bigg], \tag{16}$$

where the approximation $L+(n_b-1)l_A\approx L$ is used. From Eq. (14), the factor $(L_{m_1}L_{m_2}L_{m_2}^*/L_m)$ in Eq. (16) can be written as

$$\left(\frac{L_{m_1}L_{m_2}L_{m_2}^*}{L_m}\right)=e^{[i(L/c)(\omega_{n_1m_1}-\omega_{nm})(\eta'+1/2)]}e^{-\ln R(\eta'+1/2)}. \tag{17}$$

Now, we integrate the left- and right-hand sides of Eq. (16) with respect to η'. Using boundary conditions Eq. (15) and defining

$$\overline{f_m}=\int_{-1/2}^{1/2}d\eta'\widetilde{f}_m(\eta',\tau'),$$

$$\overline{q_m}=\int_{-1/2}^{1/2}d\eta'\widetilde{q}_m(\eta',\tau'),$$

we have

$$\frac{\partial\overline{f_m}}{\partial\tau'}=-K'(1+ia_m'-i\Delta_1')\overline{f_m}-\widetilde{R}I_pK'\overline{q_m},$$

$$\frac{\partial\overline{q_m}}{\partial\tau'}=-\left((1+i\Delta_2')\overline{q_m}+\frac{\overline{f_m}}{I_p}-\frac{1}{I_p^2}\sum_{m_1,m_2}\Gamma_{m_1m_2m_2m}C_{m_1m}\overline{f_{m_1}}|\overline{f_{m_2}}|^2\right), \tag{18}$$

where

$$C_{m_1m}=\int_{-1/2}^{1/2}d\eta' e^{[i(L/c)(\omega_{n_1m_1}-\omega_{nm})(\eta'+1/2)]}, \tag{19}$$

$K=cT/2L$, $K'=K/\gamma_\perp$, $a_m'=\delta_m/(T/2)=(\omega_{nm}-\omega_c)/K$, $\Delta_1'=(\gamma_\perp/K)\delta_1'=\delta_{sc}/K$, pump parameter $\widetilde{R}=\alpha l_A/(T/2)I_p=ibe^{-i\phi_0}$, $b=(2\pi c/\lambda K)(l_A/L)\Delta n_s$, and transmissivity of the mirror $T=1-R$. To get Eq. (18) we have made some approximations as follows. In the first approximation we carry out the uniform field limit (i.e., $T,|\alpha l_A|\ll 1$) by retaining only the first-order terms in T and αl_A, so the integration of the last factor in Eq.(16) is written approximately as

$$\frac{1}{I_p^2}\sum_{m_1,m_2}\int_{-1/2}^{1/2}d\eta'\Gamma_{m_1m_2m_2m}\left(\frac{L_{m_1}L_{m_2}L_{m_2}^*}{L_m}\right)\widetilde{f}_{m_1}|\widetilde{f}_{m_2}|^2$$
$$\approx\frac{1}{I_p^2}\sum_{m_1,m_2}\overline{f_m}|\overline{f_{m_2}}|^2\int_{-1/2}^{1/2}d\eta'\Gamma_{m_1m_2m_2m}\times e^{[i(L/c)[\omega_{n_1m_1}-\omega_{nm})(\eta'+1/2)]}.$$

In the second approximation we assume that the length of the medium l_A is far smaller than the Rayleigh length of the cavity field in the region occupied by the active medium [2], so for $-1/2\leqslant\eta'\leqslant 1/2$ we have

$$A_m(\rho,\phi,\eta')\approx A_m(\rho,\phi,0)=A_m(\rho,\phi).$$

As for $A_m(\rho,\phi)$ we choose the Gauss-Laguerre modes in this paper:

$$A_m(\rho,\phi)=A_{p,l}^{(i)}(\rho,\phi)=\frac{2}{\sqrt{\eta_1}}\left(2\frac{\rho^2}{\eta_1}\right)^{l/2}\left(\frac{p!}{(p+l)!}\right)^{1/2}\times L_p^l\left(\frac{2\rho^2}{\eta_1}\right)e^{-\rho^2/\eta_1}B_l^{(i)}(\phi),$$

$$B_l^{(i)}(\phi)=\begin{cases}\frac{1}{\sqrt{2\pi}}, & l=0\\ \frac{1}{\sqrt{\pi}}\cos l\phi, & l>0,\quad i=1\\ \frac{1}{\sqrt{\pi}}\sin l\phi, & l>0,\quad i=2\end{cases} \tag{20}$$

where $p=0,1,\ldots$ is the radial index and $l=0,1,\ldots$ is the angular index, $i=1,2$ for $l>0$. $L_p^l(2\rho^2/\eta_1)$ indicates the Laguerre polynomial of order p and l. It is obviously convenient for our calculation to eliminate the parameter η_1 in working Eq. (18), so we introduce a new radial variable $\rho'=\rho/\sqrt{\eta_1}$, and Eq. (20) becomes

$$A_{pl}^{(i)}(\rho',\phi)=\frac{1}{\sqrt{\eta_1}}\overline{A_{pl}^{(i)}}(\rho',\phi),$$

$$\overline{A_{pl}^{(i)}}(\rho',\phi)=2[2\rho'^2]^{l/2}\left(\frac{p!}{(p+l)!}\right)^{1/2}\times L_p^l(2\rho'^2)e^{-\rho'^2}B_l^{(i)}(\phi), \tag{21}$$

the coupling coefficients

$$\Gamma_{m_1m_2m_2m}=\frac{1}{\eta_1}\widetilde{\Gamma}_{m_1m_2m_2m},$$

$$\widetilde{\Gamma}_{m_1m_2m_2m}=\int_0^\infty\rho'd\rho'\int_0^{2\pi}d\phi\overline{A_{m_1}}\,\overline{A_{m_2}}\,\overline{A_{m_2}}\,\overline{A_m}(\rho',\phi). \tag{22}$$

Substituting them into Eq. (18) and defining $E_m=\overline{f_m}/\sqrt{\eta_1}\sqrt{I_p}$, $P_m=(\overline{q_m}/\sqrt{\eta_1})\sqrt{I_p},\tau'=\gamma_\perp t$, we have

$$\frac{\partial E_m}{\partial t} = -K[(g_m + i a'_m - i\Delta'_1)E_m - \tilde{R}P_m],$$
$$\frac{\partial P_m}{\partial t} = -\gamma_\perp\Bigg((1+i\Delta'_2)P_m - E_m + \sum_{m_1 m_2} \tilde{\Gamma}_{m_1 m_2 m_2 m} C_{m_1 m} E_{m_1} |E_{m_2}|^2\Bigg). \tag{23}$$

The parameter η_1 is no longer explicitly in evidence in the above equation. Equation (23) is the basic equation for the field model amplitudes and these modes may have the same longitude index or not. For convenience we list its parameters again: $K = cT/2L$ and $\gamma_\perp = 1/\tau_0$ are the relaxation rates of the oscillating field and the grating, respectively. Coefficients $g_m = 1 + d_m$, where d_m denote the diffraction losses of the different transverse modes. $a'_m = (\omega_{nm} - \omega_c)/K$, $\Delta'_1 = \delta_{sc}/K = (\omega_s - \omega_c)/K$, $\Delta'_2 = \delta_{ps}/\gamma_\perp = (\omega_p - \omega_s)/\gamma_\perp$. Pump parameter $\tilde{R} = ibe^{-i\phi_0}$ $[b = (2\pi c/\lambda K)(l_A/L)\Delta n_s]$ is generally complex and becomes real only when the dc electric field $E_0 = 0$ (i.e., $\phi_0 = \pi/2$). The $C_{m_1 m}$ and the mode-mode coupling coefficients $\tilde{\Gamma}_{m_1 m_2 m_2 m}$ are given by Eqs. (19) and (22), respectively. From Eq. (19), the magnitude of $C_{m_1 m}$ is related closely to the frequency spacing of the oscillating modes: When these modes are nondegenerate, i.e., $(\omega_{n_1 m_1} - \omega_{nm}) \gg K$, then $C_{m_1 m} = \delta_{n_1 n}\delta_{m_1 m}$. But if the oscillating modes are degenerate or quasidegenerate, i.e., $(\omega_{n_1 m_1} - \omega_{nm}) \sim K$, we have $C_{m_1 m} \approx 1$. As shown in the latter text, the behavior of the oscillator in this case is more complicated.

III. THE CHARACTERISTICS OF SINGLE-MODE OSCILLATION

As a preparation for studying multimode oscillation, the characteristics of single-mode oscillation are discussed in this section, particularly when the dc electric field $E_0 \neq 0$. For single-mode oscillation, it is convenient to choose its empty-cavity resonance frequency ω_{nm} as the reference frequency ω_c, then we have $a'_m = 0$, $\Delta'_1 = (\omega_s - \omega_{nm})/K$, and Eq. (23) can be simplified to

$$\frac{\partial E_m}{\partial t} = -K[(g_m - i\Delta'_1)E_m - \tilde{R}P_m],$$
$$\frac{\partial P_m}{\partial t} = -\gamma_\perp[(1+i\Delta'_2)P_m - E_m + \tilde{\Gamma}_{mmmm}E_m I_m], \tag{24}$$

where $I_m = E_m E_m^*$. Making $\partial E_m/\partial t = 0$, $\partial P_m/\partial t = 0$, we get the steady intensity and the corresponding frequency relation:

$$I_m^{\rm st} = \frac{1}{\tilde{\Gamma}_{mmmm}}\left(1 - \frac{g_m^2 + \Delta_1'^2}{\tilde{R}_r g_m - \tilde{R}_i \Delta'_1}\right),$$
$$\Delta'_2 = \frac{\tilde{R}_i g_m + \tilde{R}_r \Delta'_1}{\tilde{R}_r g_m - \tilde{R}_i \Delta'_1}, \tag{25}$$

where $\tilde{R}_r = b\sin\phi_0$, $\tilde{R}_i = b\cos\phi_0$ are the real and imaginary part of the pump parameter $\tilde{R}$, respectively. If we introduce the frequency difference δ between the pump beam ω_p and the empty-cavity resonance ω_{nm}, $\delta = \omega_p - \omega_{nm}$, and notice the relation $\delta = \delta_{sc} + \delta_{ps}$, we get the frequency pulling from Eq. (25):

$$\delta_{ps} = \frac{\gamma_\perp}{g_m K + \gamma_\perp}\,\delta, \quad \phi_0 = \frac{\pi}{2}, \tag{26}$$

$$\delta_{ps} = \frac{-l_2 + \sqrt{l_2^2 - 4l_1 l_3}}{2l_1}, \quad \phi_0 \neq \frac{\pi}{2}, \tag{27}$$

where

$$l_1 = \tilde{R}_i,$$
$$l_2 = \tilde{R}_r K g_m + \tilde{R}_r\gamma_\perp - \tilde{R}_i\delta,$$
$$l_3 = -(\tilde{R}_i K\gamma_\perp g_m + \tilde{R}_r\gamma_\perp\delta).$$

When the dc electric field $E_0 = 0$, from Eq. (26) we can see that the frequency pulling has the same form as that in lasers if $g_m = 1$. While in PRO the response time of the oscillating field is much shorter than that of the grating (i.e., $\gamma_\perp \ll K$), then we have $\delta_{ps} \ll \delta$ which means that the frequency pulling is very strong; but when $E_0 \neq 0$, the frequency pulling becomes complicated, as shown in Eq. (27). In this case, we give the $\delta - \delta_{ps}$ curves labeled (1), (2), (3), and (4) for A_{00} mode in Fig. 2(a), their nonlocal phase shift being $\phi_0 = \pi/2$, $2\pi/6$, $\pi/6$, and 0, respectively. The other parameters are $R = 0.8$, $L = 2$ m, $l_A = 0.02$ m, $\tau_0 = 1$ s, $\lambda = 1.0\times10^{-6}$ m, for A_{00} mode $g_m = 1$, the coefficient $\Gamma_{mmmm} = 0.3183$, and $\Delta n_s = 0.805\times10^{-6}$, 0.865×10^{-6}, 1.08×10^{-6}, and 1.63×10^{-6} corresponding to curves (1), (2), (3), and (4), respectively. In Fig. 2(a) the detuning δ for every curve is varied under the condition of $I_m^{\rm st} \geq 0$, i.e., above the oscillating threshold. With Eqs. (25)–(27), the variation for δ can be written as

$$\frac{\tilde{R}_i(\gamma_\perp - K) - \sqrt{\tilde{R}_i^2 + 4(\tilde{R}_r - 1)}(\gamma_\perp + K)}{2} \leq \delta \leq \frac{\tilde{R}_i(\gamma_\perp - K) + \sqrt{\tilde{R}_i^2 + 4(\tilde{R}_r - 1)}(\gamma_\perp + K)}{2}. \tag{28}$$

In the case of $E_0 \neq 0$, Fig. 2 (a) shows that the curve of δ_{ps} vs δ is nonlinear, and the detuning $\delta = 0$ does not mean the frequency difference δ_{ps} (between the oscillating field and the pump beam) is also equal to zero, i.e., the δ and δ_{ps} are not equal to zero at the same time. In addition, the oscillating threshold given by Eq. (28) is asymmetric with respect to $\delta = 0$. These characteristics, however, are absent when the electric field $E_0 = 0$.

Next we consider the steady intensity $I_m^{\rm st}$. Owing to our abandoning the plane-wave description, Eq. (25) for $I_m^{\rm st}$ includes the mode-mode coupling coefficients $\tilde{\Gamma}_{mmmm}$ which is the result of the transverse effect, and then the intensity of the higher-order mode will be stronger than that of the lower one if neglecting the diffraction losses, because the coupling coefficients $\tilde{\Gamma}_{mmmm}$ of the higher-order mode are smaller.

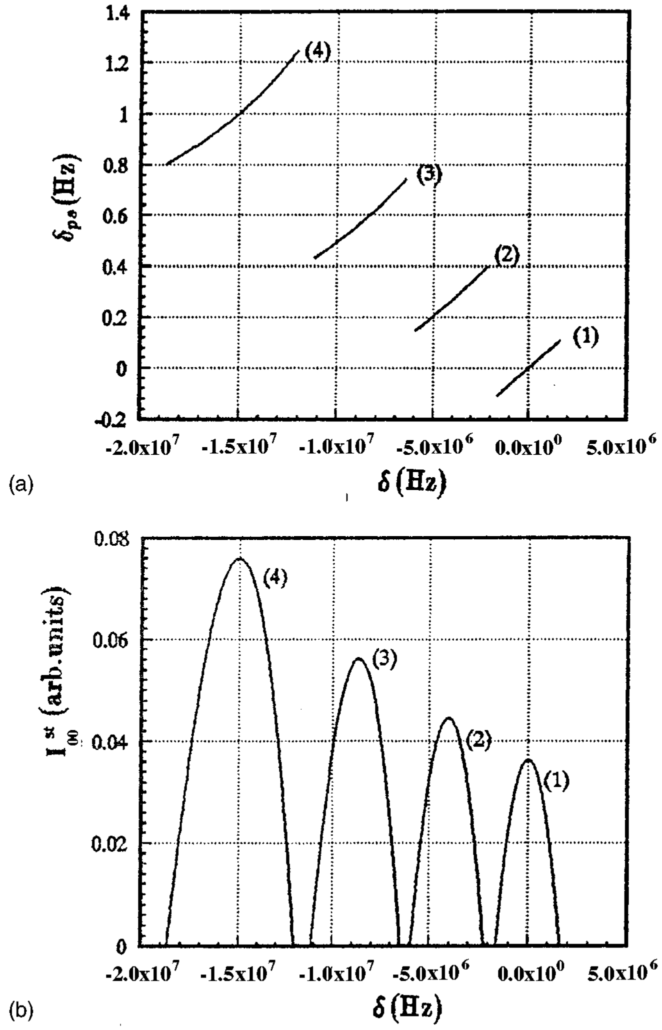

FIG. 2. Dependence of the frequency difference δ_{ps} (a) and the steady intensity I^{st}_{00} (b) on the detuning δ with the different nonlocal phase shifts (1) $\phi_0=\pi/2$, (2) $2\pi/6$, (3) $\pi/6$, and (4) 0 standing for the different dc electric fields E_0.

The reason is that the higher-order mode can take better advantage of the available gain because of its greater modal extent when the pumped region is sufficiently broad. Another characteristic of the intensity I^{st}_m is the existence of an extreme value with respect to δ_{ps} (or the detuning δ). From Eqs. (25)–(27) and relation $\delta=\delta_{sc}+\delta_{ps}$, δ_{ps} and the detuning δ corresponding to this extreme value are

$$\delta_{ps}=tg\left(\frac{\pi}{4}-\frac{\phi_0}{2}\right)\gamma_\perp,$$
$$\delta=tg\left(\frac{\pi}{4}-\frac{\phi_0}{2}\right)(\gamma_\perp-Kg_m). \tag{29}$$

When the electric field $E_0=0$, Eq. (29) indicates that the steady intensity I^{st}_m reaches its extreme value in the resonant state $\delta=0$; if $E_0\neq 0$, however, the extreme value of I^{st}_m appears in the detuning state $\delta\neq 0$ (and $\delta_{ps}\neq 0$) which means there is a moving interference pattern in the photorefractive medium [see Eq. (8)]. We know that in certain circumstances the fringe displacement will enhance the amplitude of the stationary $\pi/2$ shift component of the grating which causes the beam coupling, therefore the gain of the medium is increased. This is the reason for the extreme value of I^{st}_m at $\delta\neq 0$ in the case of $E_0\neq 0$. It can be seen more clearly in Fig. 2(b) in which we give the $\delta-I^{st}_m$ curves (1), (2), (3), and (4) for A_{00} mode-with the nonlocal phase shift $\phi_0=\pi/2$, $2\pi/6$, $\pi/6$ and 0, respectively; the other parameters are the same as in Fig. 2(a). Each curve in Fig. 2(b) has a peak value at the detuning point δ determined by Eq. (29). So far the characteristics of the single-mode oscillation under the different dc electric fields are clear.

IV. INSTABILITY OF MULTIMODE OSCILLATION

In this section we discuss multimode oscillation, and the modes operating in degenerate or quasidegenerate states are studied carefully by numerical simulation. As mentioned above, there is a relation $K\gg\gamma_\perp$ in PRO, so it is reasonable to adiabatically eliminate the field by making $\partial E_m/\partial t\approx 0$ in Eq. (23), and have

$$E_m=(A_m+iB_m)P_m, \tag{30}$$

where

$$A_m=\frac{\widetilde{R}_r g_m-\widetilde{R}_i\Delta'_m}{g_m^2+\Delta'^2_m},$$

$$B_m=\frac{\widetilde{R}_i g_m+\widetilde{R}_r\Delta'_m}{g_m^2+\Delta'^2_m},$$

$\Delta'_m=\Delta'_1-a'_m=(\omega_s-\omega_{nm})/K$. With the relation Eq. (30), Eq. (23) for P_m becomes

$$\frac{\partial P_m}{\partial t}=-\gamma_\perp\Bigg((1+i\Delta'_2)P_m-(A_m+iB_m)P_m + \sum_{m_1,m_2}\widetilde{\Gamma}_{m_1m_2m_2m}C_{m_1m}(A_{m_1}+iB_{m_1})D_{m_2}\widetilde{I}_{m_2}P_{m_1}\Bigg),$$

$$D_m=A_m^2+B_m^2,\quad \widetilde{I}_m=P_mP_m^*. \tag{31}$$

This is the equation for describing the multimode oscillation in the photorefractive oscillator.

For simplicity, we consider a three-mode oscillation,

$$\overline{A_{00}}(\rho',\phi)=\frac{2}{\sqrt{2\pi}}e^{-\rho'^2},$$

$$\overline{A_{01}}(\rho',\phi)=\frac{2}{\sqrt{\pi}}(2\rho'^2)^{1/2}e^{-\rho'^2}\cos\phi, \tag{32}$$

$$\overline{A_{02}}(\rho',\phi)=\frac{2}{\sqrt{\pi}}(2\rho'^2)\left(\frac{1}{2!}\right)^{1/2}e^{-\rho'^2}\cos 2\phi.$$

These modes have different angular but the same radial index ($p=0$); for convenience, we only write out the angular index l for the mode index m in the following. From Eqs. (22) and (32), we can get the mode-mode coupling coefficients $\Gamma_{m_1m_2m_2m}$:

$$\begin{bmatrix} \tilde{\Gamma}_{0000} & \tilde{\Gamma}_{0001} & \tilde{\Gamma}_{0002} \\ \tilde{\Gamma}_{1000} & \tilde{\Gamma}_{1001} & \tilde{\Gamma}_{1002} \\ \tilde{\Gamma}_{2000} & \tilde{\Gamma}_{2001} & \tilde{\Gamma}_{2002} \end{bmatrix} = \begin{bmatrix} 0.3183 & 0.0000 & 0.0000 \\ 0.0000 & 0.1592 & 0.0000 \\ 0.0000 & 0.0000 & 0.0796 \end{bmatrix},$$

$$\begin{bmatrix} \tilde{\Gamma}_{0110} & \tilde{\Gamma}_{0111} & \tilde{\Gamma}_{0112} \\ \tilde{\Gamma}_{1110} & \tilde{\Gamma}_{1111} & \tilde{\Gamma}_{1112} \\ \tilde{\Gamma}_{2110} & \tilde{\Gamma}_{2111} & \tilde{\Gamma}_{2112} \end{bmatrix} = \begin{bmatrix} 0.1592 & 0.0000 & 0.0796 \\ 0.0000 & 0.2387 & 0.0000 \\ 0.0796 & 0.0000 & 0.1194 \end{bmatrix},$$

$$\begin{bmatrix} \tilde{\Gamma}_{0220} & \tilde{\Gamma}_{0221} & \tilde{\Gamma}_{0222} \\ \tilde{\Gamma}_{1220} & \tilde{\Gamma}_{1221} & \tilde{\Gamma}_{1222} \\ \tilde{\Gamma}_{2220} & \tilde{\Gamma}_{2221} & \tilde{\Gamma}_{2222} \end{bmatrix} = \begin{bmatrix} 0.0796 & 0.0000 & 0.0000 \\ 0.0000 & 0.1194 & 0.0000 \\ 0.0000 & 0.0000 & 0.1790 \end{bmatrix}. \tag{33}$$

We know that the nonzero elements of the coupling coefficients are corresponding to a kind of interaction among the modes which makes the behavior of the oscillator more complicated, but from Eq. (31) whether these interactions really operate or not is also dependent on another parameter $C_{m_1 m}$. If the oscillating modes are nondegenerate, we have $C_{m_1 m} = \delta_{n_1 n}\delta_{m_1 m}$; this means that the modes interact with each other only by the terms of $\Sigma_{m_2}\tilde{\Gamma}_{mm_2m_2m}E_m(A_m + iB_m)D_{m_2}\tilde{I}_{m_2}P_m$ [see Eq. (31)] which can be regarded as the contribution from the diagonal elements of the coupling coefficients, Eq. (33). In fact, these terms describe the mode competition and in this case Eq. (31) can be simplified to the Lotka-Volterra equation:

$$\frac{\partial \tilde{I}_m}{\partial t'} = \alpha_m \tilde{I}_m - \sum_{m'} Q_{mm'}\tilde{I}_{m'}\tilde{I}_m ,$$

$$\alpha_m = A_m - 1, \quad Q_{mm'} = \tilde{\Gamma}_{mm'm'm}D_{m'}A_m , \quad t' = 2\gamma_\perp t$$

which indicates the multimode oscillation in nondegenerate states will be stable after a competition process. In this paper, however, we discuss emphatically a degenerate or quasidegenerate case, therefore $C_{m_1 m} \approx 1$, which leads to the mode-mode interaction terms $\Sigma_{m_1 m_2}\tilde{\Gamma}_{m_1m_2m_2m}(A_{m_1} + iB_{m_1})D_{m_2}\tilde{I}_{m_2} \times P_{m_1}$ $(m_1 \neq m)$ resulting from the nondiagonal elements of coupling coefficients operating in addition to the mode competition terms $\Sigma_{m_2}\tilde{\Gamma}_{mm_2m_2m}(A_m + iB_m)D_{m_2}\tilde{I}_{m_2}P_m$, and we expect rich spatiotemporal phenomena are the results of these additional interactions. If we introduce $P_m = X_m + iY_m$, Eq. (31) becomes

$$\frac{\partial X_m}{\partial \tau} = \Bigg((A_m - 1)X_m + (\Delta_2' - B_m)Y_m - \sum_{m_1, m_2} \tilde{\Gamma}_{m_1m_2m_2m}D_{m_2}\tilde{I}_{m_2}(A_{m_1}X_{m_1} - B_{m_1}Y_{m_1}) \Bigg), \tag{34}$$

$$\frac{\partial Y_m}{\partial \tau} = \Bigg((B_m - \Delta_2')X_m + (A_m - 1)Y_m - \sum_{m_1, m_2} \tilde{\Gamma}_{m_1m_2m_2m}D_{m_2}\tilde{I}_{m_2}(B_{m_1}X_{m_1} + A_{m_1}Y_{m_1}) \Bigg),$$

$$\tilde{I}_m = X_m^2 + Y_m^2, \quad \tau = \gamma_\perp t$$

where index $m = 0,1,2$ indicates the three different transverse modes given by Eq. (32). Equation (34) is the basic equation for our numerical simulation, and we integrate it with the Runge-Kutta method. In the simulation, the parameters Δ_2' and Δ_m' (i.e., Δ_{00}', Δ_{01}', Δ_{02}') are given by the following considerations only for convenience: We choose the empty-cavity resonance frequency of $A_{00}(\rho', \phi)$ mode ω_{00} as the reference frequency ω_c, so $\Delta_{00}' = \Delta_1' - a'_{00} = \Delta_1'$. While the Δ_1' and Δ_2' are determined in the case of single-mode $[A_{00}(\rho', \phi)]$ oscillation in the best state, which means that the detuning δ is satisfied to Eq. (29), and Δ_2', Δ_1' can be given by

$$\Delta_2' = tg\left(\frac{\pi}{4} - \frac{\phi_0}{2}\right),$$
$$\Delta_1' = \Delta_{00}' = \left[tg\left(\frac{\pi}{4} - \frac{\phi_0}{2}\right)\right] g_{00}. \tag{35}$$

Then Δ_{01}', Δ_{02}' can be determined around Δ_{00}' if we realize that the difference among them indicates the frequency spacing of these modes. The only point we need pay attention to is the difference $(\Delta_{m_1}' - \Delta_{m_2}') \not\gg 1$ in degenerate or quasidegenerate states.

The case of dc electric field $E_0 = 0$ is studied first, i.e., the nonlocal phase shift $\phi_0 = \pi/2$. From Eq. (35) we obtain $\Delta_2' = \Delta_{00}' = 0$. The other parameters are reflectivity $R = 0.8$, cavity length $L = 2$ m, medium length $l_A = 0.02$ m, delay time $\tau_0 = 1$ s, wavelength $\lambda = 1.0 \times 10^{-6}$ m, diffraction losses $d_{00} = 0.0$, $d_{01} = 2.8 \times 10^{-3}$, $d_{02} = 8.0 \times 10^{-3}$, and the saturation value of the photoinduced index change $\Delta n_s = 0.82 \times 10^{-6}$, while the parameters of Δ_{01}' and Δ_{02}' are variable to change the frequency spacing among the modes. When $\Delta_{01}' = \Delta_{02}' = 0$, Fig. 3(a) gives relative intensity of each mode varying with the time. It shows that the modes become stable after competing. If $\Delta_{01}' = 4.0 \times 10^{-3}$, $\Delta_{02}' = 8.0 \times 10^{-3}$; however, the system becomes unstable as shown in Fig. 3(b) in which the intensity of each mode appears as a periodic fluctuation with a large amplitude, and the intensity variations of the A_{00} and A_{02} modes are in phase but out of phase with the A_{01} mode, i.e., we can observe the A_{00} and A_{02} modes appear simultaneously but alternately with the A_{01} mode. Increasing the frequency spacing, $\Delta_{01}' = 3.0 \times 10^{-2}$, $\Delta_{02}' = 6.0 \times 10^{-2}$, different from Fig. 3(b), the intensity fluctuation of the modes decreases as shown in Fig. 3(c), which means the mode-mode interaction is weaker than that in Fig. 3(b). In addition, the time unit in the figures indicates that the instability phenomenon is a slowly varying behavior.

Next, we simulate the three-mode oscillation when the dc electric field $E_0 \neq 0$, and assuming $\phi_0 = 0$. Therefore we have $\Delta_2' = 1$, $\Delta_{00}' = g_{00}$ from Eq. (35). The other parameters are the

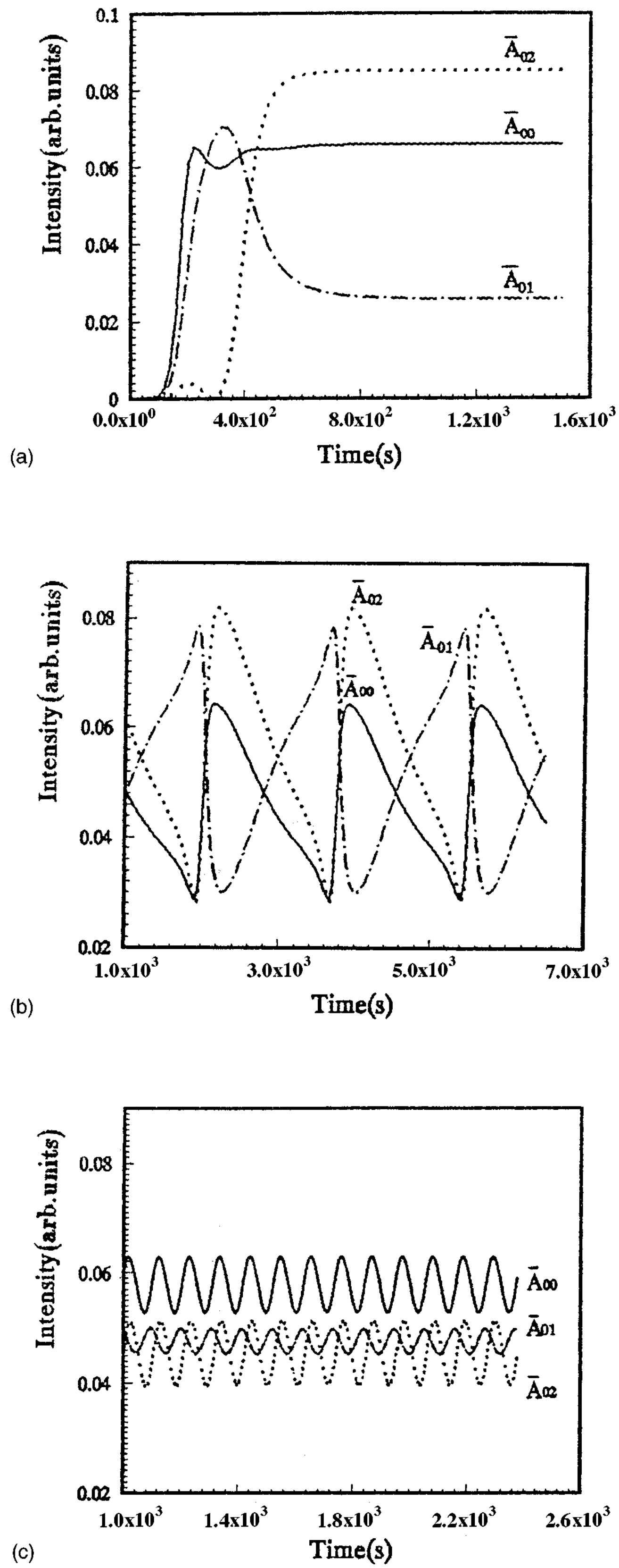

FIG. 3. Normalized intensity of the modes $\overline{A_{00}}$, $\overline{A_{01}}$, and $\overline{A_{02}}$, as a function of time (second) in the case of $E_0=0$ (i.e., $\phi_0=\pi/2$). The frequency difference parameters (a) $\Delta'_{01}=\Delta'_{02}=0$, (b) $\Delta'_{01}=4.0\times10^{-3}$, $\Delta'_{02}=8.0\times10^{-3}$, and (c) $\Delta'_{01}=3.0\times10^{-2}$, $\Delta'_{02}=6.0\times10^{-2}$.

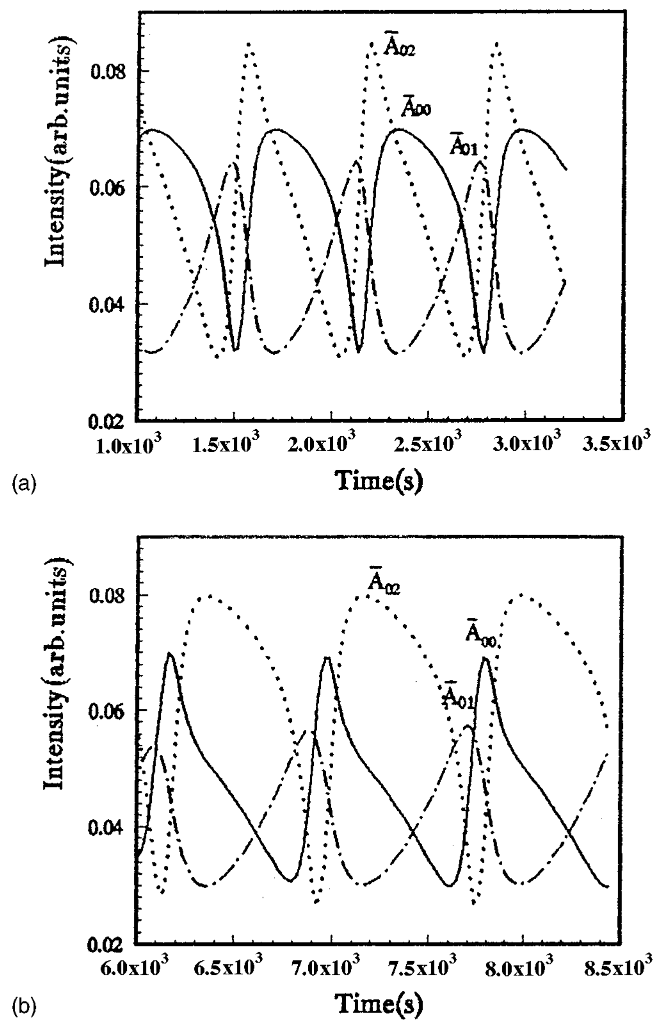

FIG. 4. Same as in Fig. 3, but the dc electric field $E_0\neq0$ and corresponding nonlocal phase shift $\phi_0=0$. The frequency difference and diffraction loss parameters are $\Delta'_{01}=1.011$, $\Delta'_{02}=1.022$, $d_{00}=0.0$, $d_{01}=3.0\times10^{-3}$, $d_{02}=7.3\times10^{-3}$ for (a) and $\Delta'_{01}=0.9984$, $\Delta'_{02}=0.9968$, $d_{00}=0.0$, $d_{01}=4.8\times10^{-3}$, $d_{02}=10.0\times10^{-3}$ for (b).

same as the above except $\Delta n_s=1.64\times10^{-6}$, $d_{00}=0.0$, $d_{01}=3.0\times10^{-3}$, $d_{02}=7.3\times10^{-3}$. With the parameters Δ'_{01}, Δ'_{02} increasing, the variation process of the system is similar to that of $E_0=0$: When $\Delta'_{01}=\Delta'_{02}=1.0$, the system is stable; while $\Delta'_{01}=1.011$, $\Delta'_{02}=1.022$, the intensity of each mode as shown in Fig. 4(a) fluctuates largely with the time, but the variation of A_{00} mode is no longer in phase with that of A_{02} as in Fig. 3(b). Therefore, in this case, we will observe a periodic alternation behavior in which each mode oscillates one after another in a regular periodic sequence, from Fig. 4(a) its sequence is $A_{00}\rightarrow A_{01}\rightarrow A_{02}\rightarrow A_{00}$. Moreover, this sequence is variable, for example, when we change the parameters $d_{00}=0.0$, $d_{01}=4.8\times10^{-3}$, $d_{02}=10.0\times10^{-3}$, $\Delta'_{01}=0.9984$, $\Delta'_{02}=0.9968$, the sequence as shown in Fig. 4(b) becomes $A_{00}\rightarrow A_{02}\rightarrow A_{01}\rightarrow A_{00}$, reversing with that in Fig. 4(a).

These results show that the additional mode couplings corresponding to the nondiagonal elements of the coupling coefficients indeed make the dynamics of the photorefractive oscillator more complicated. This fact indicates that some more complicated spatiotemporal phenomena such as spatiotemporal quasiperiodic behavior and spatiotemporal chaos will possibly appear when the number of oscillating modes increases.

V. CONCLUSION

We have developed a theory for multimode oscillation in a photorefractive ring oscillator in the weak-field limit. Applying the theory to single-mode oscillation, we obtained some characteristics of steady intensity and frequency pulling under different dc electric fields, When the field $E_0=0$, the frequency difference δ_{ps} (between pump and signal beams) varies with the detuning δ linearly, and the intensity attains its maximum value at $\delta=0$. But if $E_0\neq0$, the variation of δ_{ps} with the detuning δ is nonlinear, and the maximum intensity appears at the detuning state $\delta\neq0$. In the case of multimode oscillation, for simplicity, we studied the three-mode oscillation by numerical simulation. The results show that the system is unstable in certain circumstances because of the additional mode-mode interactions in degenerate or quasidegenerate states. Instabilities such as the periodic alternation phenomenon are observed, and the dc electric field E_0 can affect its alternation sequence.

ACKNOWLEDGMENTS

We are grateful to Dr. Zhu Jianqiang for assistance in computation and to Dr. Ma Guobin for useful discussions.

[1] W. Klische, C. O. Weiss, and B. Wellegehausen, Phys. Rev. A **39**, 919 (1989).
[2] L. A. Lugiato, G. L. Oppo, J. R. Tredicce, L. M. Narducci, and M. A. Pernigo, J. Opt. Soc. Am. B **7**, 1019 (1990).
[3] L. A. Lugiato, F. Prati, L. M. Narducci, P. Ru, J. R. Tredicce, and D. K. Bandy, Phys. Rev. A **37**, 3847 (1988).
[4] M. Brambilla, F. Battipede, L. A. Lugiato, V. Penna, and F. Prati, Phys. Rev. A **43**, 5090 (1991).
[5] E. M. Wright, W. J. Firth, and I. Galbraith, J. Opt. Soc. Am. B **2**, 383 (1985).
[6] P. Colet, M. San Miguel, M. Brambilla, and L. A. Lugiato, Phys. Rev. A **43**, 3862 (1991).
[7] A. Kummorov, Opt. Commun. **96**, 185 (1993).
[8] F. T. Arecchi, G. Giacomelli, P. L. Ramazza, and S. Residori, Phys. Rev. Lett. **65**, 2531 (1990).
[9] F. T. Arecchi, G. Giacomelli, P. L. Ramazza, and S. Residori, Phys. Rev. Lett. **67**, 3794 (1991).
[10] Daniel Hennequin, Laurent Dambly, Didier Dangoisse, and Pierre Glorieux, J. Opt. Soc. Am. B **11**, 676 (1994).
[11] G. D'Alessandro, Phys. Rev. A **46**, 2791 (1992).
[12] Pochi Yeh, J. Opt. Soc. Am. B **2**, 1924 (1985).
[13] Laurent Dambly and Hassina Zeghlache, Phys. Rev. A **49**, 4043 (1994).
[14] Dana Z. Anderson, J. Opt. Soc. Am. B **4**, 164 (1987).
[15] P. Coullet, L. Gil, and F. Rocca, Opt. Commun. **73**, 403 (1989).
[16] C. O. Weiss, H. R. Telle, K. Staliunas, and M. Brambilla, Phys. Rev. A **47**, 1616 (1993).
[17] J. P. Huignard and A. Marrakchi, Opt. Commun. **38**, 249 (1981).
[18] A. Marrakchi and J. P. Huignard, Appl. Phys. **24**, 131 (1981).